# Fabrication and Characterization of Thermo-pneumatic Peristaltic Micropumps

Hsin-Hung Liao and Yao-Joe Yang

Department of Mechanical Engineering,
National Taiwan University, Taipei, Taiwan
TEL: +886-2-33662712 Email: yjy@ntu.edu.tw

## ABSTRACT

In this paper, the fabrication and characterization of thermopneumatic peristaltic micropumps are presented. Micropumps with three different designs are fabricated using soft lithography techniques. The optimal operating conditions, such as duty ratios, operating frequencies and backpressure, are obtained. The maximum flow rate occurs at a driving frequency of 1.5Hz with a duty ratio of 40%. Under zero backpressure, the maximum flow rates of the 3, 5 and 7-chamber devices are very close, while the devices with larger numbers of pumping chambers exhibit better pumping performance under higher backpressure.

***Keywords***: peristaltic micropump, thermopneumatic, MEMS, microfluidics, PDMS

## 1 INTRODUCTION

Microfluidic systems, realized by MEMS technologies, are widely employed for many biomedical applications. The advantages of these microfluidic devices include high throughput, rapid response, small size, low cost, low power consumption and reduction in reagents. In each microfluidic system, micropumps usually serve as the key components to drive and control small volumes of chemical and biological working fluids. For displacement micropumps [1], periodical volume strokes of fluids are generated by using existing actuating mechanisms to push or pull one or more moveable boundaries. The actuating mechanisms include piezoelectric [2], electromagnetic [3], electrostatic [4], pneumatic [5], thermopneumatic [6,7], and so on. One of the most popular types of displacement micropump is the peristaltic-type pump. A peristaltic micropump generates peristaltic motions of the diaphragms, which are arranged in series, for squeezing the fluid in a desired direction.

The actuation mechanism using thermopneumatic principle can generate large deflections of diaphragms with relatively low driving voltages and simple driving sequences. Therefore, a microsystem which employs thermopneumatic mechanism potentially can be realized in a very small package. Furthermore, thermopneumatic actuators can be easily fabricated by soft lithography micromachining process [8]. In this work, we fabricate and characterize three types of peristaltic micropumps based on the thermopneumatic mechanism. We will also measure the pumping performances of the devices, including the relationship between flow rate vs. duty ratio, the relationship between the flow rate vs. driving frequency (under zero backpressure), and the relationship between the flow rate vs. backpressure.

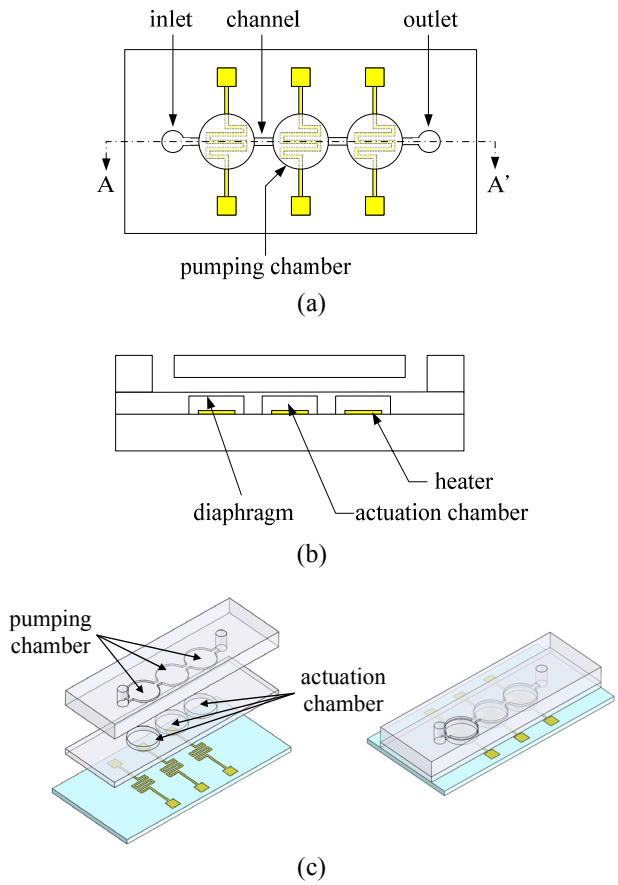


Figure 1. The schematic view of the micropump: (a) top view; (b) cross-sectional view; (c) 3D schematic illustration.

## 2 DESIGN

Figure 1 shows the schematic of the peristaltic micropump with three pumping chambers (the 3-chamber device). The micropump consists of three different layers: the channel layer, the chamber layer and the heater layer. The channel layer and the chamber layer are fabricated with PDMS elastomer, whereas the heater layer is realized by patterning metal film on a glass substrate. When the voltage is applied to the heater, the temperature of the air

inside the *actuation chamber* increases, and consequently the air volume expands and the diaphragm is deformed to squeeze the fluid in the *pumping chamber*. As the temperature of the air inside the actuation chamber reduces due to natural cooling, the air volume decreases and the deformation of the diaphragm decreases. Figure 2 shows the working principles of the actuation sequences studied in this work. By controlling the movement of the diaphragms in sequence, the fluid can be conveyed.

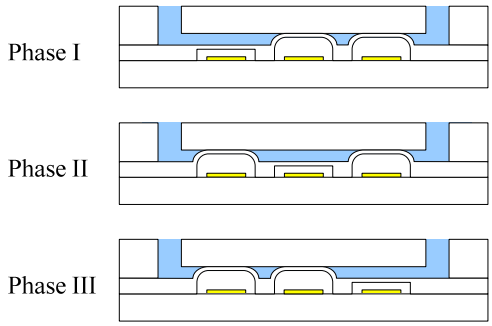


Figure 2. The actuation sequence for the peristaltic micropump.

## 3 FABRIACATION PROCESS

Figure 3 shows the fabrication process of the micropump. The channel and chamber layers are fabricated with PDMS by soft lithography technology. Figure 3(a)-3(d) show the fabrication process of the channel layer. PDMS prepolymer and curing agent (Sylgard® 184, Dow Corning Corp.) are mixed at 10:1 ratio. After stirred thoroughly and degassed in a vacuum chamber, the prepared PDMS mixture is poured onto a patterned SU-8 master (GM 1070, Gersteltec Sarl) of 50 μm-thick (Figure 3(a)-3(b)). After cured at 90°C for 60 min, the cured PDMS layer is peeled off from the master substrate (Figure 3(c)). The through-holes for the inlet and the outlet are punched using stainless steel pipe (Figure 3(d)). The chamber layer can be fabricated by the similar process, as shown in Figure 3(e)-3(g). The patterned SU-8 master is 180 μm in thickness (Figure 3(e)). Since the thickness of the chamber layer has to be controlled around 230 μm, the prepared PDMS mixture is poured and spun at 300 rpm for 10 sec (Figure 3(f)). After softly cured at 90°C for 30 min, the chamber layer is peeled off from the master (Figure 3(g)).

Figure 3(h)-3(j) show the fabrication process of the heater layer. A lift-off process is employed. Thick positive photoresist (AZ4620, Hoechst) is spin-coated (5,000 rpm, 50sec) and patterned on a glass wafer (Corning® 1737) (Figure 3(h)). A 200Å thick titanium and 3000Å thick gold layer is deposited by electron beam evaporation, then the heater pattern is formed by removing the photoresist (Figure 3(i)-3(j)).

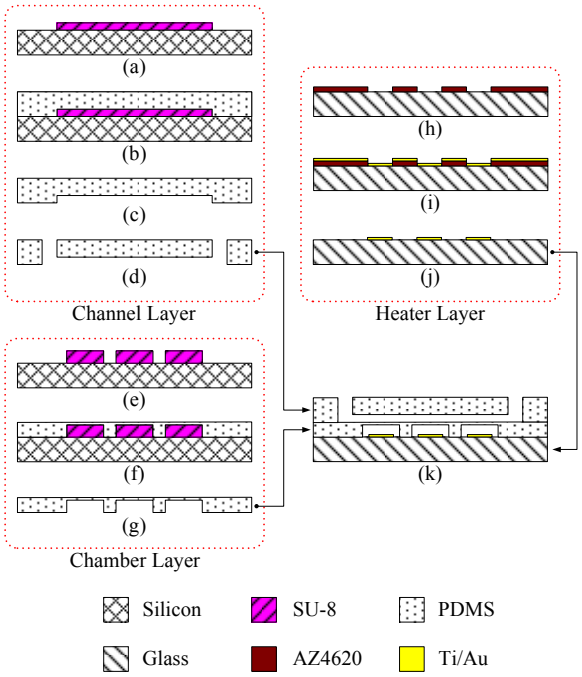


Figure 3. The fabrication process of the micropump.

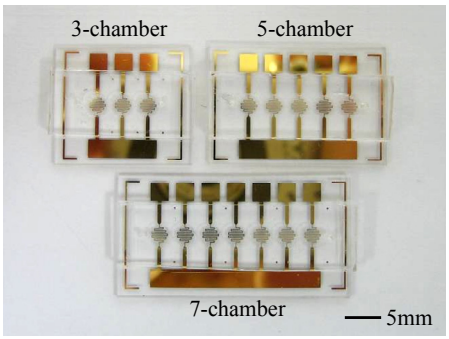


(a)

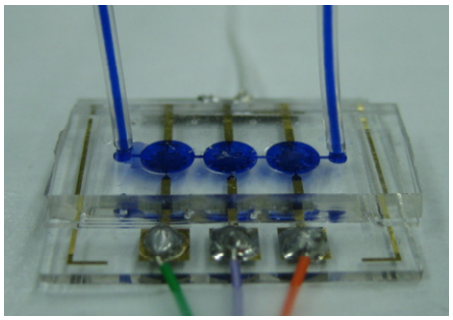

(b)

Figure 4. The photograph of the fabricated micropump: (a) the 3-chamber, 5-chamber, and 7-chamber micropumps; (b) the micropump after connecting polyethylene tube.

After oxygen plasma treatment (pressure 350 mTorr, RF Power 10.5W, 90 sec.), the channel layer and the chamber layer are bonded and then cured at 80°C for 5 minutes. The heater layer is also bonded to the other side of chamber layer after the similar oxygen plasma treatment (Figure 3(k)). Finally, polyethylene (PE) tubes are connected to the inlet/outlet and electrical wires are soldered on the pads of the heaters. Figure 4(a) shows the picture of the fabricated 3-chamber, 5-chamber and 7-chamber micropumps. Figure 4(b) is a 3-chamber device connected with PE tubes

.

## 4 EXPERIMENT AND RESULTS

Figure 5 shows the schematic of the experiment setup for measuring the flow rates of the micropump. The inlet and the outlet of the micropump are connected to reservoirs using polyethylene tubes (PE20, I.D. 0.38 mm, O.D. 1.09 mm, INTRAMEDIC®). The de-ionized water is used as the working fluid for the experiments. By controlling $\Delta h$ shown in the figure, the backpressure between inlet and outlet can be adjusted. The heating voltage for each heater is controlled by a FET switch, which receives the time sequences generated by a PC-based data acquisition card.

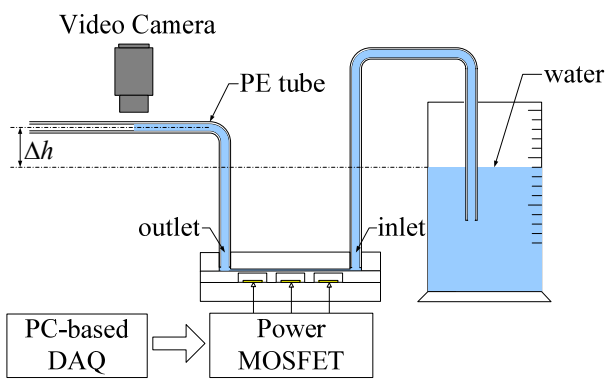


Figure 5. The setup for the measurement of the flow rates of the micropump.

Note that in the following experiments, the applied voltage to the heater inside the thermopneumatic actuation cell is fixed at 5V. The meniscus displacement of the fluid in the tube that is connected to the outlet is recorded by a video camera with a macro lens. From the meniscus displacement, the flow rate is able to be calculated.

Figure 6 shows the timing diagrams of the actuation sequence. In each actuation cycle, the time period $T$ is evenly divided into *three* phase durations ($T_{phase}$). The duty ratio is defined as:

$$D = \frac{T_{heat}}{T_{phase}} \quad (\%) \qquad (1)$$

where $T_{phase}$ is the time duration of each phase, and $T_{heat}$ is the heating time in the duration. Both $T_{phase}$ and $T_{heat}$ are indicated in Figure 6. Note that the driving frequency $f$ is equal to $1/T$ .

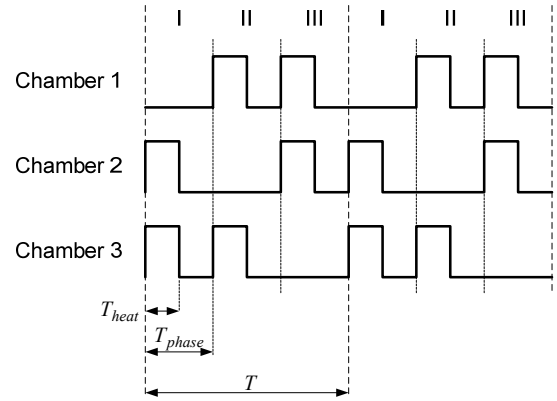


Figure 6. The timing diagram of the actuation sequence.

Figure 7 shows the measured flow rate versus the duty ratio for the 3-chamber device, under the condition of zero backpressure (i.e., $\Delta h = 0$ in Figure 5). As the driving frequency is either 1Hz or 2Hz, the maximum flow rate occurs when the duty ratio is about 40%.

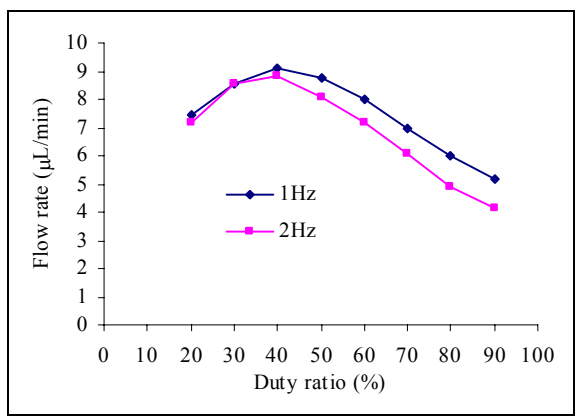


Figure 7. The measured flow rate vs. duty ratio.

Figure 8 shows the measured flow rate versus the frequency for the 3-chamber, 5-chamber and 7-chamber micropumps under zero backpressure. At low frequency (i.e., less than 1.5Hz), the flow rate increases with the frequency. However, the flow rate starts to decrease as frequency is greater than 1.5Hz. It is because the actuation amplitude of the diaphragm decreases with frequency due to insufficient heating. The measured maximum flow rate of these three types of micropumps occurs around 1.5Hz. The corresponding maximum flow rates for these three types of devices are very close. These results indicate that the flow rate of the micropumps is not affected by the numbers of the serial pumping chambers.

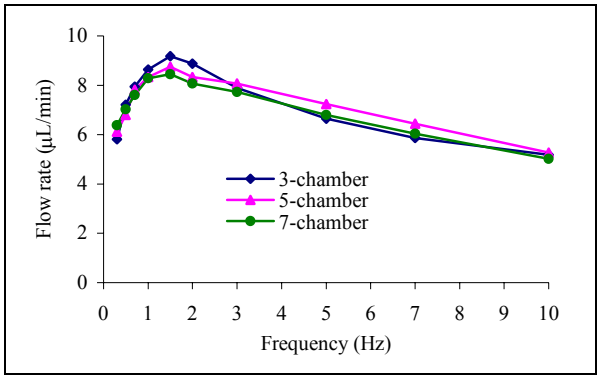


Figure 8. The measured flow rate vs. frequency for three different devices.

Figure 9 shows the measured relationship between the backpressure and the flow rate at 1.5Hz. The flow rate decreases linearly as the backpressure increases. In other words, the pumps with larger numbers of chambers exhibit better pumping flow rates under higher backpressure. The phenomenon can be explained by the numbers of *actuated pumping chambers* for each device during operation. The *actuated pumping chamber* is the pumping chamber which is under heating so that its diaphragm is deformed and the fluid inside the chamber is squeezed out. During operation, the pump with larger number of *actuated pumping chambers* has higher flow impedance, so it can resist higher backpressure. Obviously, the device with larger number of pumping chambers has larger number of *actuated pumping chambers*, so it has better pumping flow rates under backpressure.

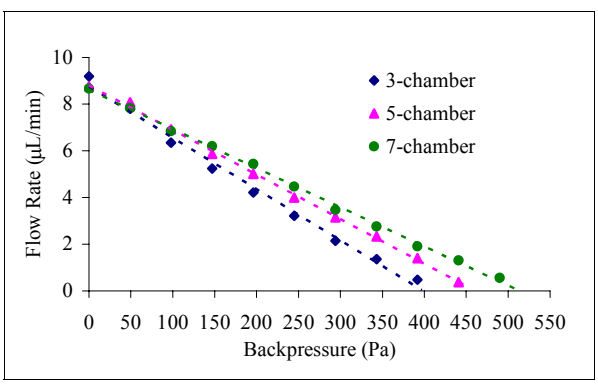


Figure 9. The measured flow rate vs. backpressure for three different devices.

## 5 CONCLUSIONS

In this work, the design, fabrication and measurement of thermopneumatic peristaltic micropump systems were presented. Micropumps with 3, 5 and 7 serial pumping chambers were fabricated using the soft lithography techniques. The pump systems can be operated with 5V input voltage. The optimal operating conditions, such as operating frequencies, backpressure and duty ratios, were obtained. The maximum flow rate occurs at the driving frequency of 1.5 Hz with a duty ratio of 40%. The pumps with larger numbers of pumping chambers have better pumping performance under the condition of higher backpressure. The advantages of the proposed micropump include simple design, easy fabrication, low operating voltage and biological compatibility.

## ACKNOWLEDGEMENT

The authors would like to thanks Prof. Lung-Jieh Yang, Tamkang University (TKU) MEMS group, for providing manufacturing process equipments.

## REFERENCES

[1] D. J. Laser and J. G. Santiago, "A review of micropumps," *Journal of Micromechanics and Microengineering*, Vol. 14, 2004, pp. 35-64

[2] L. S. Jang, Y. J. Li, S. J. Lin, Y. C. Hsu, W. S. Yao, M. C. Tsai and C. C. Hou, "A stand-alone peristaltic micropump based on piezoelectric actuation," *Biomedical Microdevices*, Vol. 9, 2007, pp. 185-194

[3] S. Haeberle, N. Schmitt, R. Zengerle and J. Ducrée, "Centrifugo-magnetic pump for gas-to-liquid sampling," *Sensors and Actuators A*, Vol. 135, 2007, pp. 28-33

[4] A. Machauf, Y. Nemirovsky and Uri Dinnar, "A membrane micropump electrostatically actuated across the working fluid," *Journal of Micromechanics and Microengineering*, Vol. 15, 2005, pp. 2309-2316

[5] O. C. Jeong and S. Konishi, "Fabrication and drive test of pneumatic PDMS micro pump," *Sensors and Actuators A*, Vol. 135, 2007, pp. 849-856

[6] W. Inman, K. Domansky, J. Serdy, B. Owens, D. Trumper and L. G. Griffith, "Design, modeling and fabrication of a constant flow pneumatic micropump," *Journal of Micromechanics and Microengineering*, Vol. 17, 2007, pp. 891-899

[7] O. C. Jeong, S. W. Park, S. S. Yang and J. J. Pak, "Fabrication of a peristaltic PDMS micropump," *Sensors and Actuators A*, Vol. 123-124, 2005, pp. 453-458

[8] Y. Xia and G. M. Whiteside, "Soft lithography," *Angewandte Chemie International Edition*, Vol. 37, 1998, pp. 550-575